Geochemistry 80 (2020) 125613

Contents lists available at ScienceDirect

Geochemistry

journal homepage: www.elsevier.com/locate/chemer

Habitability of hydrothermal systems at Jezero and Gusev Craters as constrained by hydrothermal alteration of a terrestrial mafic dike

Lacey J. Costello[a,1], Justin Filiberto[b,*], Jake R. Crandall[c], Sally L. Potter-McIntyre[a], Susanne P. Schwenzer[d], Michael A. Miller[e], Daniel R. Hummer[a], Karen Olsson-Francis[d], Scott Perl[f]

[a] Southern Illinois University, Department of Geology, 1259 Lincoln Drive, Carbondale, IL, 62901, USA
[b] Lunar and Planetary Institute, USRA, 3600 Bay Area Blvd., Houston, TX, 77058, USA
[c] Eastern Illinois University, Department of Geology and Geography, Physical Science Building, 600 Lincoln Ave., Charleston, IL, 61920, USA
[d] School of Environment, Earth, and Ecosystems Sciences, The Open University, Walton Hall, Milton Keynes, MK7 6AA, UK
[e] Materials Engineering Department, Southwest Research Institute, 6220 Culebra Road, San Antonio, TX, 78238, USA
[f] Jet Propulsion Laboratory, California Institute of Technology, 4800 Oak Grove Dr, Pasadena, CA, 91109-8001, USA

ARTICLE INFO

Handling Editor: Astrid Holzheid

Keywords:
Hydrothermal
Mars alteration
Terrestrial analog
Gusev Crater
Jezero Crater
NE Syrtis

ABSTRACT

NASA's search for habitable environments has focused on alteration mineralogy of the Martian crust and the formation of hydrous minerals, because they reveal information about the fluid and environmental conditions from which they precipitated. Extensive work has focused on the formation of alteration minerals at low temperatures, with limited work investigating metamorphic or high-temperature alteration. We have investigated such a site as an analog for Mars: a mafic dike on the Colorado Plateau that was hydrothermally altered from contact with groundwater as it was emplaced in the porous and permeable Jurassic Entrada sandstone. Our results show evidence for fluid mobility removing Si and K but adding S, Fe, Ca, and possibly Mg to the system as alteration progresses. Mineralogically, all samples contain calcite, hematite, and kaolinite; with most samples containing minor anatase, barite, halite, and dolomite. The number of alteration minerals increase with alteration. The hydrothermal system that formed during interaction of the magma (heat source) and groundwater would have been a habitable environment once the system cooled below ~120 °C. The mineral assemblage is similar to alteration minerals seen within the Martian crust from orbit, including those at Gusev and Jezero Craters. Therefore, based on our findings, and extrapolating them to the Martian crust, these sites may represent habitable environments which would call for further exploration and sample return of such hydrothermally altered igneous materials.

1. Introduction

There is extensive evidence for water activity on ancient Mars from orbital investigations of geomorphic features (fluvial valleys, outflow channels, fans, deltas, paleolakes, lobate craters) (Carr, 1996; Carr and Head, 2010; Lasue et al., 2019) and in situ rover investigations of ancient sedimentary rocks and structures (conglomerates and mudstones, grain size sorting, cross bedding, and rounding of pebbles) (McLennan, 2012; Williams et al., 2013). Diverse alteration minerals have been discovered in the Martian crust from orbit (Ehlmann and Edwards, 2014), in Martian meteorites (Treiman et al., 1993; Bridges et al., 2001, 2019), as well as in situ from rover investigations (Arvidson and Catalano, 2018; Jolliff et al., 2019; Mittlefehldt et al., 2019; Sutter et al., 2019). Clay minerals are predominantly found in the ancient Noachian and possibly into the early Hesperian crust preserving evidence of weathering, hydrothermal activity, and diagenesis (Mustard et al., 2008; Ehlmann and Edwards, 2014). Localized carbonates and chlorides have been found within paleolake deposits (Ehlmann et al., 2008) including the deltaic deposit in Jezero Crater (Goudge et al., 2015; Salvatore et al., 2018), which was chosen as the landing site for the NASA Mars 2020 rover. Possible evidence for hydrothermal activity in the form of silica, hematite, and sulfate sand, as well as localized carbonate deposits, were also investigated by MER Spirit at Gusev Crater (Morris et al., 2010; Filiberto and Schwenzer, 2013; Ruff and

* Corresponding author.
E-mail address: JFiliberto@lpi.usra.edu (J. Filiberto).
[1] Now at Jacobs JETS, NASA Johnson Space Center, Houston, TX 77058, USA.

https://doi.org/10.1016/j.chemer.2020.125613
Received 31 October 2019; Received in revised form 26 February 2020; Accepted 27 February 2020

Farmer, 2016). Furthermore, two groups of Martian meteorites, the nakhlites and orthopyroxenite ALH84001, contain carbonates that record evidence of alteration (Bridges et al., 2001; Bridges and Schwenzer, 2012; Bridges et al., 2019). At more recent times in Martian history a predominance of sulfates and iron-oxides in crustal deposits analyzed from orbit (Bibring et al., 2006; Ehlmann and Edwards, 2014) suggests a drying out of the surficial part of the crust.

The Martian crust is primarily basaltic in composition (McSween et al., 2003; Ehlmann and Edwards, 2014; Filiberto, 2017), thus the observed alteration minerals have formed from a mafic protolith in a variety of conditions (pressure, temperature, and fluid composition). To understand reaction pathways, terrestrial analogue studies for basalt alteration have largely focused on palagonite formation in Hawaii and Iceland (Morris et al., 2001; Bishop et al., 2002). Palagonite typically forms by alteration and hydration of basaltic glass at high water to rock ratios to form an alteration gel or fibrous material with clays, zeolites, oxides and carbonates precipitating in pore space (Stroncik and Schmincke, 2002). However, both sites (Hawaii and Iceland) are dominated by alteration of mafic glasses through interaction with seawater (Staudigel and Hart, 1983; Drief and Schiffman, 2004), which is not a process found to date on Mars (Banin and Margulies, 1983). Further, extensive work has focused on either modeling or experimentally investigating low temperature alteration (e.g., Griffith and Shock, 1995, 1997; Zolotov and Mironenko, 2007; McAdam et al., 2008; Schwenzer and Kring, 2009; Marion et al., 2011; Filiberto and Schwenzer, 2013; Schwenzer and Kring, 2013; Melwani Daswani et al., 2016; Zolotov and Mironenko, 2016; Hurowitz et al., 2006; Tosca and McLennan, 2009), with fewer studies focusing on higher temperature metamorphic conditions or magmatic hydrothermal systems (e.g., Schulze-Makuch et al., 2007; McCubbin et al., 2009; Filiberto et al., 2014; McCanta et al., 2014; McSween, 2015; Ruff and Farmer, 2016; Semprich et al., 2019).

Therefore, we have investigated the mineral assemblage and bulk chemistry changes that occur from in situ hydrothermal alteration of a mafic dike with groundwater on the Colorado Plateau. Our results allow us to predict what constraints this interaction can place on habitability of this environment as well as similar environments on Mars – specifically at Gusev Crater and the regional area around Jezero Crater in North East Syrtis.

1.1. Geologic background

On and near the Colorado Plateau in south-central Utah, hundreds of mafic dikes were emplaced into Jurassic sedimentary rocks, at the eastern limit of the Tertiary volcanic field (Delaney and Gartner, 1997). Our investigation focuses on the 22 Ma Robbers Roost dike, located at 38°30′58.52″N, 110°26′32.57″W, which is exposed several kilometers east of the main cluster of dikes (Wannamaker et al., 2000). The dike is a light rare earth element enriched olivine-phlogopite-lamproite that intruded pre-existing northwest oriented fracture systems in the crust (Wannamaker et al., 2000). The dike intruded through the Jurassic Entrada Sandstone of the San Rafael Group, an iron-cemented red silty-sandstone (Crabaugh and Kocurek, 1993). The Entrada varies regionally between siltstone and sandstone of various proportions, and exposures to the West of the Green River differ significantly from exposures east of the river. In the San Rafael Swell, the Entrada Sandstone is mostly very fine grained sandstone to siltstone with four partly crossbedded sandstone units (Wright et al., 1979; O'Sullivan, 1981).

1.2. Field description

The dike can be separated into four visually distinct zones based on differences in colors and textures presumably correlated to different degrees of alteration (Fig. 1). The region of the intrusion located at the far northwest limit of the exposure is the freshest in appearance and darkest in color. The next distinct zone is yellow-green in coloration and is overall more friable than the other three sections. Continuing to the southeast, the intrusion is a deep purple-red color. The final zone of the dike lies at the southeastern extent of the exposed intrusion and is of bright crimson color. The surrounding sandstone is preferentially harder than the dike with the darkest zone of the dike being the most consolidated and resistant to weathering. The purple and red zones of the dike are increasingly less weathering resistant and thus of rubbly and weathered appearance. The green zone is the most rubbly in appearance, represents the smallest portion of the exposure, and the outcrop itself is the least continuous.

2. Methods

For bulk chemistry, one representative aliquot from each section of the intrusion (dark, green, purple, and red; Fig. 2) was powdered and sent to the Southwest Research Institute in San Antonio (SWRI®). The bulk powder was analyzed semi-quantitatively using an IXRF Systems (Model 550i) energy dispersive X-ray spectrometer (EDS) attached to a Philips (Model XL-40) scanning electron microscope. Samples were analyzed in scanning mode using low magnification (100-300x) and a ~1 μm beam to ensure that the relative elemental abundancies determined from the integrated X-ray detector counts for each element of interest were representative of the bulk powder. The relative concentrations were calculated according to the well-known k-ratio protocol, wherein corrections for atomic number, absorption, and secondary fluorescence are accounted (Reed and Ware, 1972; Lifshin et al., 1975; Fiori et al., 1976). The linearity of the EDS detector response as a function of elemental abundance (~0.1 to 16 wt.%) was verified by analyzing a series of NBS-certified standard reference materials (SRM 1193, 1194, and 1195, National Bureau of Standards), each one consisting of different absolute concentrations of the elements: Mn, P, S, Si, Cu, Cr, V, Mo, Ti, Al, and Zr in a balance of Fe. Further, three different areas were analyzed to ensure that the EDS spectrum was consistent for each sample. The overall error relative to SRM values for all elemental components was estimated to be ± 8%.

For mineral analyses (bulk mineralogy and clay fraction), samples from each zone of the dike (n = 4) were disaggregated and analyzed using X-Ray Diffraction (XRD) with a Rigaku Ultima IV at Southern Illinois University. All samples (bulk and clay fractions) were analyzed with a Cu rotating anode (1.54 Å wavelength), 40 kV, 44 mA, a sampling interval of 0.02 degrees, and a scan speed of 0.6 s/step. Random powdered samples were analyzed for bulk mineralogy between 5 and 65° 2-theta.

Oriented clay fraction (< 2 μm) samples were analyzed between 2 and 35° 2-theta. To make the clay fraction analyses, powders from each zone were mixed with 100 mL of water and 10 mL of 5% solution trisodium phosphate to peptize the sample. This mixture was then run through an Eppendorf centrifuge at 1000 rpm for 5 minutes. The supernatant was reserved and centrifuged again at 4000 rpm for an additional 4 minutes. The remaining slurry was smeared onto a glass slide, air-dried, and analyzed.

Materials Data Inc. (MDI) Jade-2010 software was used to interpret XRD patterns and identify minerals present in samples for both bulk and clay fraction analyses. Data were treated conservatively; tentatively identified phases, potentially consistent with just one peak or peak shoulder, were not listed as present in Table 2.

Bulk uncut rock samples (n = 4) were analyzed by visible to near-infrared reflectance spectroscopy (VNIR) using the hand held probe attached to an ASD TerraSpec Pro spectrometer at Southern Illinois University to obtain mineralogy observations comparable to orbital and lander VNIR data for the Martian crust. This instrument measures wavelengths between 350 and 2500 nm. The resolution of the instrument is 3 nm at 700 nm and 6 nm at 1400/2100 nm. Samples were prepared by breaking open fresh surfaces. They were analyzed at room temperature, using a contact probe where the spectrometer was placed directly against the flattest surface. The resulting spectra were analyzed

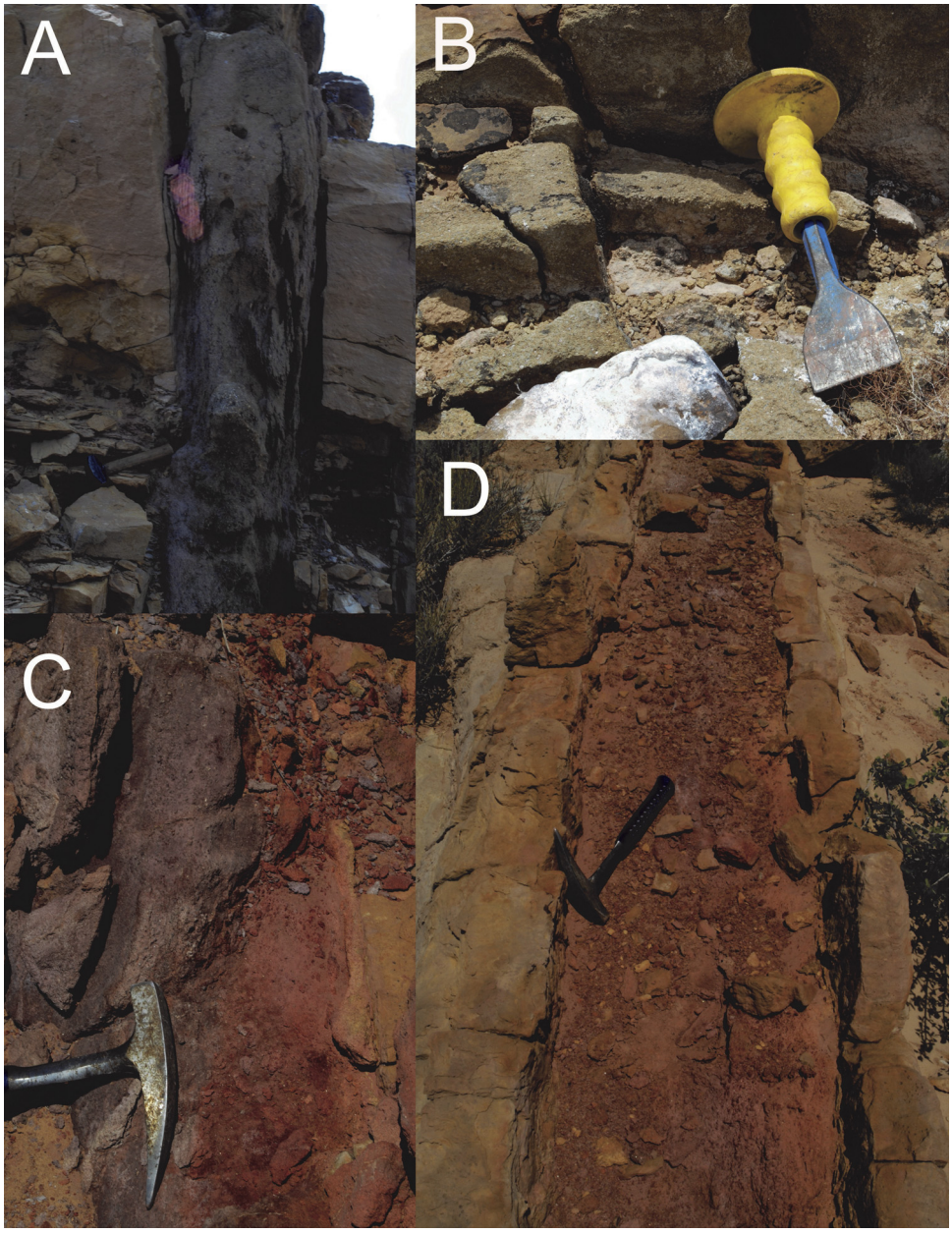

Fig. 1. Field site showing each of the four visually distinct alteration zones of the dike. The alteration and oxidation of the dike changes from the 'darkest' zone (a), the 'green' zone (b), the 'purple' zone (c), and the 'red' zone (d). The dike exhibits increasing oxidation from zone a through d. Hammer and chisel for scale. (For interpretation of the references to colour in this figure legend, the reader is referred to the web version of this article).

using The Spectral Geologist (TSG™) software version 8 to identify minima at wavelengths that indicate specific minerals.

3. Results

3.1. Chemistry

Bulk chemistry has been measured and results are presented normalized to the darkest sample (presumed to be the least altered) to emphasize how the bulk chemistry changes with alteration (Table 1; Fig. 3). All three alteration zones are depleted in silicon, potassium, and manganese, and enriched in sulfur and calcium compared to the darkest sample. Sulfur increases while potassium and silicon decrease moving from the NW to the SE along the dike, consistent with an increase in alteration minerals. Both the purple and red samples are enriched in iron compared to the darkest sample. Aluminum, chromium, titanium, and phosphorous displayed no systematic changes and can be considered immobile in the system within the uncertainty of our measurements (note that for the red sample all values are slightly below one which is caused by the large sulfur, calcium, and magnesium influx and not necessarily by removal of these elements). This is consistent with fluid mobility removing Si and K but adding S, Fe, Ca, and possibly Mg presumably from the surrounding rock. However, the low-energy photons of Mg suffer much higher absorption compared to the high-energy photons of the heavier elements captured at the detector of the XRF EDS and therefore there is larger uncertainty in the measurement. We note, that the chemistry of the green dike is somewhat different from the other three, which we attribute to the larger amount of calcite in that sample compared with the rest (see the following Mineralogy section); thus, increasing the Ca content of the rock and decreasing several other elements (including iron) accordingly.

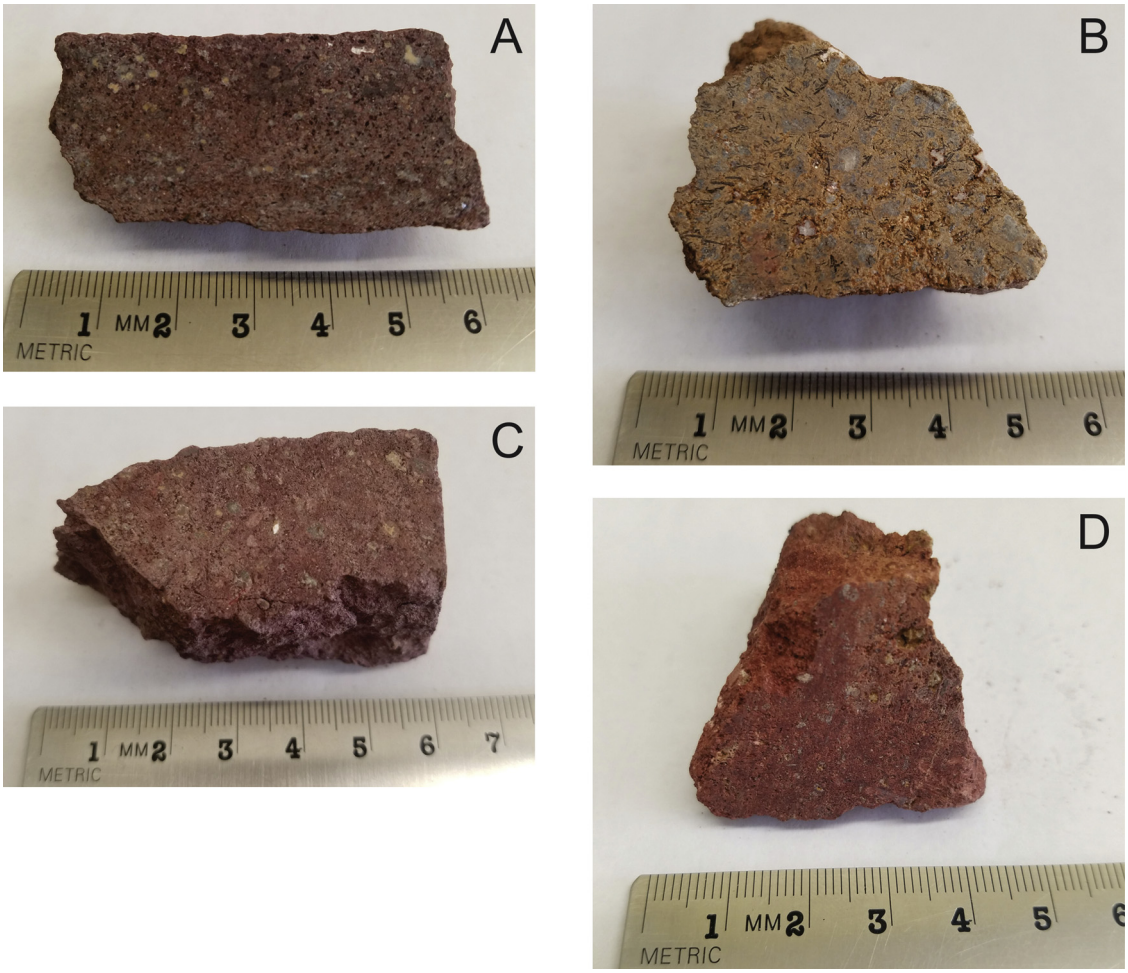

Fig. 2. Hand samples with fresh cut surfaces of different regions of the dike: a) dark, b) green, c) purple, and d) red. All samples show some alteration but with increasing oxidation/alteration going from A to D. (For interpretation of the references to colour in this figure legend, the reader is referred to the web version of this article).

Table 1
Bulk chemistry of each sample.

	Dark	Green	Purple	Red
Na	N.D.	N.D.	1.06	1.63
Mg	3.91	1.32	3.26	6.19
Al	13.18	14.78	14.59	11.73
Si	27.54	25.76	21.02	19.36
P	1.91	2.34	1.66	1.56
S	0.68	1.01	0.87	2.80
K	6.17	5.74	2.61	2.52
Ca	14.03	34.43	14.37	19.60
Ti	5.77	7.45	5.17	4.53
Cr	0.28	0.36	0.23	0.23
Mn	0.36	0.33	0.29	0.23
Cl	N.D.	N.D.	1.78	1.02
Fe	26.17	6.50	33.11	28.62
	100.00	100.00	100.00	100.00

N.D. Not detected.

3.2. Mineralogy

Mineralogy of all samples is consistent between measurement techniques (XRD and VNIR) with the differences being attributed to the sensitivity of the technique (Table 2). All samples contain phlogopite, which is from the igneous protolith. The only other igneous minerals found in all samples are sanidine-high and apatite. Even the least altered sample shows significant amounts of alteration minerals and while the crystal molds of former olivine are visible in hand sample (Fig. 2), olivine is not detected in any sample. Instead, all samples contain calcite, hematite, and kaolinite. Most samples also contain anatase, barite, halite, and dolomite. Kaolinite is present in all zones of the dike. Goethite, palygorskite and halloysite only formed in the most altered sample. The number of alteration phases increase in abundance with increasing alteration (Fig. 4; Table 1). The red sample has the most alteration phases including gypsum and the lowest abundance of primary igneous minerals.

4. Discussion

4.1. Conditions of alteration

Extensive previous work on thermochemical modeling of alteration mineralogy can provide constraints on the temperature, pH, and water to rock ratio during alteration (McAdam et al., 2008; Schwenzer and Kring, 2009; Filiberto and Schwenzer, 2013). Carbonates in our samples point to a near neutral pH and CO_2-bearing fluid (Bridges et al., 2019). Focusing on modeling results of neutral pH fluids can then be used to constrain temperature evolution of the system (e.g., Filiberto and Schwenzer, 2013). In order for Si to be mobile in a near-neutral pH fluid, high temperatures (> 200 °C) would be required (Filiberto and Schwenzer, 2013; Ruff and Farmer, 2016). Therefore, the system started at high temperatures with the magma intruding the sandstone causing a hydrothermal system at near-neutral pH and a dilute fluid

Table 2
Mineralogy of each sample by technique and grain size.

Sample	Technique		Mineralogy								
Dark	VNIR	Bulk	Phlogopite	Calcite	Kaolinite	Hematite	Fluorapatite	Sanidine-High	Anatase	Barite	Gypsum
	XRD	Bulk	Phlogopite	Calcite	Kaolinite	Hematite					
		< 2 μm fraction	Phlogopite		Kaolinite						
Green	VNIR	Bulk	Phlogopite	Calcite	Kaolinite	Hematite					
	XRD	Bulk	Phlogopite	Calcite	Kaolinite	Hematite (+Magnetite)					
		< 2 μm fraction	Phlogopite	Calcite	Kaolinite		Fluorapatite	Sanidine-High	Anatase		
Purple	VNIR	Bulk	Phlogopite	Calcite	Kaolinite	Hematite	Goethite				
	XRD	Bulk	Phlogopite	Calcite	Kaolinite	Hematite		Fluorapatite	Sanidine-High	Anatase	Barite
		< 2 μm fraction			Kaolinite						
Red	VNIR	Bulk	Phlogopite	Calcite	Kaolinite	Hematite	Goethite				
	XRD	Bulk	Phlogopite	Calcite	Kaolinite	Hematite	Goethite	Fluorapatite	Sanidine-High	Anatase	Barite
		< 2 μm fraction	Phlogopite	Calcite	Kaolinite (+ Halloysite)						

Sample	Technique		Mineralogy								
Dark	VNIR	Bulk	Phlogopite	Calcite	Kaolinite	Hematite					
	XRD	Bulk	Phlogopite	Calcite	Kaolinite	Hematite					
		< 2 μm fraction	Phlogopite		Kaolinite						
Green	VNIR	Bulk	Phlogopite	Calcite	Kaolinite	Hematite					
	XRD	Bulk	Phlogopite	Calcite	Kaolinite	Hematite (+Magnetite)					
		< 2 μm fraction	Phlogopite	Calcite	Kaolinite		Fluorapatite	Sanidine-High	Anatase		
Purple	VNIR	Bulk	Phlogopite	Calcite	Kaolinite	Hematite	Goethite				
	XRD	Bulk	Phlogopite	Calcite	Kaolinite	Hematite		Fluorapatite	Sanidine-High	Anatase	Barite
		< 2 μm fraction			Kaolinite						
Red	VNIR	Bulk	Phlogopite	Calcite	Kaolinite	Hematite	Goethite				
	XRD	Bulk	Phlogopite	Calcite	Kaolinite	Hematite	Goethite	Fluorapatite	Sanidine-High	Anatase	Barite
		< 2 μm fraction	Phlogopite	Calcite	Kaolinite (+ Halloysite)						

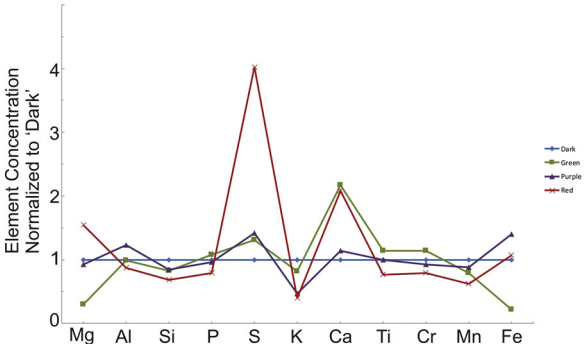

Fig. 3. Bulk rock chemistry from each zone normalized to the 'darkest' zone of the dike. Values less than one indicate elements that have been depleted compared with the least altered sample and therefore were removed from the system during alteration, while values greater than one indicate elements that are enriched compared to the darkest sample and are therefore added to the bulk chemistry of the system during alteration.

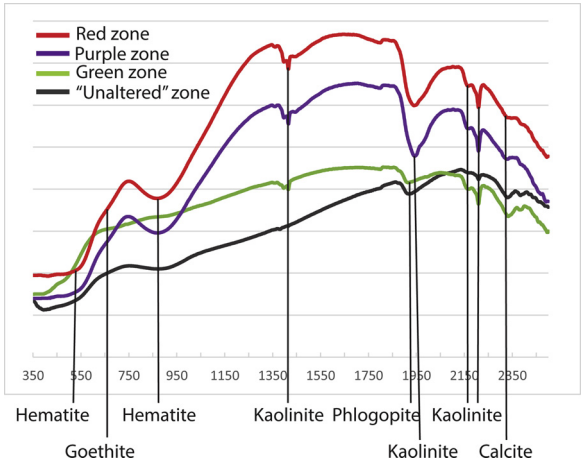

Fig. 4. Stacked VNIR reflectance spectroscopy data from each of the four zones of the dike. Moving from top to bottom, these zones include the 'darkest' zone (a), the 'green' zone (b), the 'purple' zone (c), and the 'red' zone (d). Shape of the minima show alteration minerals. (For interpretation of the references to colour in this figure legend, the reader is referred to the web version of this article).

before cooling to produce the rest of the mineral assemblage (Fig. 5). The presence of carbonates, kaolinite, and hematite suggests high water to rock ratios, temperatures ≥150 °C, and > 0 but < 0.5 mol CO_2 based on models for alteration at Gusev Crater, Mars (Filiberto and Schwenzer, 2013). Higher CO_2 concentrations would produce more carbonates but destabilize hematite, and low CO_2 concentrations would not produce carbonates. Goethite would be produced at lower temperatures but still with a high water to rock ratios as the hydrothermal system cools. Finally, the presence of the clay minerals halloysite and palygorskite in the most altered sample are indicative of the extended circulation of hot brines with high concentrations of Mg and Si (Birsoy, 2002), and gypsum and halite would only precipitate from the fluid at the very end from a more concentrated brine.

4.2. Applications to Gusev Crater

At Gusev Crater, MER Spirit analyzed a potential hot spring and/or hydrothermal deposit (Schmidt et al., 2008; Yen et al., 2008; Filiberto and Schwenzer, 2013; Ruff and Farmer, 2016). The mineralogy of the area in Gusev Crater is quite similar to what we have found at the Colorado Plateau (Table 1): Sulfate sands at Paso Robles, Dead Sea, Shredded, Arad, Tyrone, and Troy; hematite-rich outcrops between

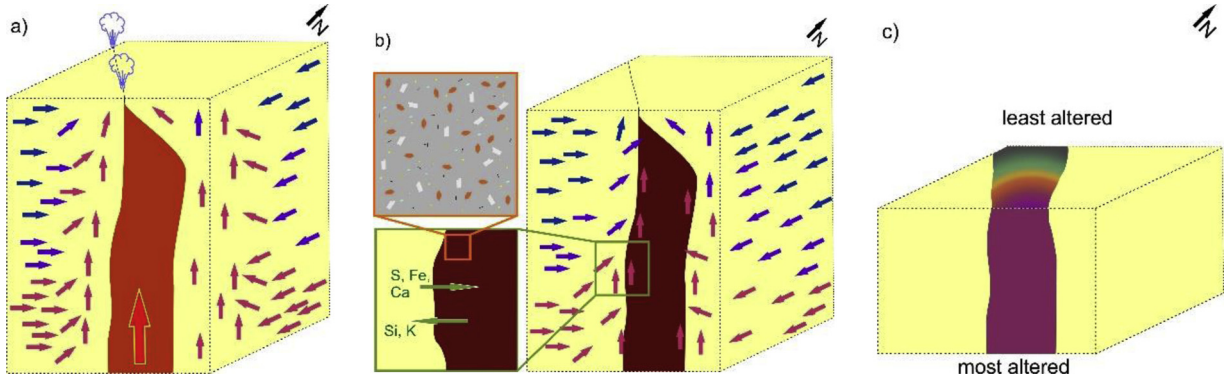

Fig. 5. The fluid history of the dike/water interaction during/after dike emplacement within the sandstone. Note that this figure focuses on the reactions in the dike. (A) Intrusion of the dike into the sandstone producing a hydrothermal system circulating through the sandstone and penetrating the dike after cooling below its ductile temperature and fracture formation; (B) shows the system as the dike and fluids cool. Green arrows indicate element mobility. Red arrows represent hot fluids, while blue arrows represent cold fluids. Orange sub-box shows the alteration minerals forming within the dike: yellow squares represent phlogopite, white laths represent feldspar altering to kaolinite, brown rhombohedra represent olivine casts, light blue represents calcite, and black lines represent oxide minerals; (C) shows the dike system after erosion and how it appears today – colors correspond to coloration of the dike shown in Fig. 1. (For interpretation of the references to colour in this figure legend, the reader is referred to the web version of this article).

Home Plate and Tyrone; SiO_2-rich deposits at Northern Valley, Eastern Valley, and Tyrone; carbonate outcrops at Comanche in the Columbia Hills; and potentially kaolinite at Wooly Patch (Morris et al., 2006; Clark et al., 2007; Morris et al., 2008; Wang et al., 2008; Yen et al., 2008; Arvidson et al., 2010; Morris et al., 2010; Ruff et al., 2011), which is consistent with relatively high water:rock ratios (such as those examined here) (Schmidt et al., 2008; Filiberto and Schwenzer, 2013; Ruff and Farmer, 2016). High-sanidine, found in all of our dike samples, has also been identified via XRD at Gale crater (Treiman et al., 2016), lending further support to the similarity of the altered K-rich igneous rocks on Mars and the present analogue site. Further, CRISM spectra showed kaolin minerals (probably (Al)-Halloysite) and carbonates within Gusev crater (Carter and Poulet, 2012). Comparing the mineralogy to Robbers Roost Dike, the clay-oxide-salt assemblage of varying abundances suggests a progressively more intense alteration with oxidation of the igneous minerals (now no longer present) and precipitation of secondary minerals. Such reaction pathways have generally been interpreted as habitable via former fluid activity owing to the availability of metabolic energy from redox reactions, and biomass increases in the subsurface by two orders of magnitude at redox fronts – particularly in high porosity settings (Cockell et al., 2009; Magnabosco et al., 2018). Additionally, these mineral assemblages in Martian (meteorite) compositions suggest circumneutral fluid conditions (Bridges and Schwenzer, 2012). Therefore, our analogue site suggests that settings of basaltic intrusions into sedimentary rocks – with or without sulfate – are ideal exploration targets, since assessing habitability has been a mission goal for all rovers and is a cornerstone for both astrobiology and human ISRU applications.

4.3. Applications to Jezero Crater, NE Syrtis, and the 'Midway' point

While we await a Mars 2020 landing in Jezero Crater, the mineralogy analyzed in the orbital data at Jezero and the surrounding NE Syrtis region is consistent with the results presented here. Jezero Crater contains a delta with strong evidence for carbonates associated with olivine (Goudge et al., 2015) and hydrated minerals. There is a potential volcanic floor unit in contact with sedimentary rocks (Goudge et al., 2015), which is where Mars 2020 will presumably land. The floor unit, if it represent a lava flow, could have formed a hydrothermal system with the sedimentary rocks below if they contained hydrated minerals, ground water, or the cryosphere. If this system formed, it could have been potentially similar to the Robbers Roost Dike field site, with the caveat that the Robbers Roost dike is a vertical dike system vs. a potentially thin horizontal volcanic floor unit (Goudge et al., 2015). Such magma driven hydrothermal systems are more common in plutonic or intrusive systems (e.g., Hochsetin and Browne, 2000), lava flows on Earth can produce similar hydrothermal systems to plutonic systems by dehydrating the substrate material (e.g., Griffiths, 2000; Hochstein and Browne, 2000). Dehydration of the substrate material could lead to melting of that substrate unit, which would then potentially cause thermal erosion (Griffiths, 2000). Therefore, geometry can affect specifics of the system, but should not substantially affect the mineralogical, geochemical, and habitability potential applicability of our results (e.g., Hochstein and Browne, 2000). What is more likely to change the outcome of such a contact in producing a hydrothermal system is the temperature and thickness of the lava flow and the nature (consolidated vs unconsolidated, anhydrous vs carbonaceous vs hydrate) of the sediments the lava contacts (Griffiths, 2000). At this point, those remain unknowns until Mars 2020 Rover lands in Jezero Crater and explores this important contact.

The larger regional area (NE Syrtis and Midway point) contains spectral signatures of olivine, pyroxene, smectite clays, sulfates, and carbonates (Ehlmann and Mustard, 2012; Goudge et al., 2015; Salvatore et al., 2018). The region has a proposed volcanic capping unit directly in contact with sulfate-bearing sediments (Goudge et al., 2015; Salvatore et al., 2018), where hydrothermal alteration from contact between these units should occur due to remobilization of S, H_2O, and/or CO_2 and, if it does, would have produced a habitable environment similar to the Robbers Roost Dike field site. Therefore, this site is an ideal analogue environment for informing site exploration of the crater floor once the rover lands, as well as a potential extended mission to the crater rim or the 'Midway' point, which is proposed to have similar geology and mineralogy to the broader NE Syrtis region (Bramble et al., 2018; Mustard et al., 2018).

4.4. Habitability of fluids

If the requirements for life on Earth are any measure for potential life on Mars, a habitable environment requires liquid water, nutrients, an energy source, and protection from detrimental influences such as a cold, highly oxidizing conditions, and high flux of ionizing radiation (Conrad, 2014). Based on that assumption, the hydrothermal system formed during interaction of the magma (heat source) and groundwater would have been a habitable environment once the system cooled below ~120 °C (Rothschild and Mancinelli, 2001; Mancinelli et al., 2004; DasSarma, 2006). The fluid entering the system would have contained C, S, and Fe, which are all key bio-essential elements, and could potentially be used as an energy source for chemolithotrophic

(Westall et al., 2015; Price et al., 2018) microorganisms (microorganisms that obtain their energy from the oxidation of reduced inorganic compounds), which could utilize the carbon to produce complex organic molecules from inorganic molecules (Cockell et al., 2016). Therefore, it is paramount that future missions look at the interface of sedimentary rocks with magmas (or impact melts), where microbial or cellular life, if present, could have taken advantage of a selection of favorable temperatures with guaranteed liquid water on a frozen planet. Moreover, active redox processes, geochemical gradients, and a moving water column to bring fresh fluid and take waste away, whilst being protected from the detrimental conditions at the Martian surface, would be an ideal in situ location for sample analyses. Further, such hydrothermally altered igneous samples should be targeted for sample caching by Mars 2020 as they represent a previously habitable environment that could preserve ancient Martian biosignatures, assuming there had been previous life.

CRediT authorship contribution statement

Lacey J. Costello: Writing - original draft, Formal analysis, Investigation, Visualization, Validation. **Justin Filiberto:** Conceptualization, Validation, Investigation, Data curation, Writing - review & editing, Supervision, Project administration, Funding acquisition. **Jake R. Crandall:** Conceptualization, Validation, Investigation, Writing - review & editing. **Sally L. Potter-McIntyre:** Conceptualization, Validation, Investigation, Data curation, Writing - review & editing, Funding acquisition. **Susanne P. Schwenzer:** Conceptualization, Investigation, Data curation, Writing - review & editing, Funding acquisition. **Michael A. Miller:** Validation, Investigation, Writing - review & editing, Formal analysis, Resources. **Daniel R. Hummer:** Validation, Investigation, Writing - review & editing, Resources. **Karen Olsson-Francis:** Writing - review & editing. **Scott Perl:** Writing - review & editing.

Declaration of Competing Interest

The authors declare that they have no known competing financial interests or personal relationships that could have appeared to influence the work reported in this paper.

Acknowledgements

The authors are appreciative of constructive comments from the D. Mittlefehldt and M.C. McCanta, as well as efficient handling by A. Holzheid. JF, SPS, JRC, and SPM would like to thank support for the initial field season from National Geographic Grant 9779-15. JF, SPM, JRC, and SP acknowledge support from NASA PSTAR grant # 80NSSC18K1686. All data are provided in Tables 1 and 2. This is LPI contribution number 2323.

References

Arvidson, R.E., Catalano, J.G., 2018. Martian Habitability As Inferred From Landed Mission Observations, From Habitability to Life on Mars. Elseviesr, pp. 77–126.
Arvidson, R.E., et al., 2010. Spirit Mars Rover Mission: overview and selected results from the northern Home Plate Winter Haven to the side of Scamander crater. J. Geophys. Res. 115, E00F03.
Banin, A., Margulies, L., 1983. Simulation of Viking biology experiments suggests smectites not palagonites, as martian soil analogues. Nature 305 (5934), 523.
Bibring, J.-P., et al., 2006. Global mineralogical and aqueous mars history derived from OMEGA/Mars express data. Science 312 (5772), 400–404.
Birsoy, R., 2002. Formation of sepiolite-palygorskite and related minerals from solution. Clays Clay Miner. 50 (6), 736–745.
Bishop, J.L., Schiffman, P., Southard, R., 2002. Geochemical and mineralogical analyses of palagonitic tuffs and altered rinds of pillow basalts in Iceland and applications to Mars. Geol. Soc. London Spec. Publ. 202 (1), 371–392.
Bramble, M.S., Mustard, J., Kremer, C.H., 2018. Geological Continuity Between the Midway and NE Syrtis candidate Landing Sites for the Mars 2020 Rover Mission. Fourth Landing Site Workshop for the Mars 2020 Rover Mission.
Bridges, J.C., Schwenzer, S.P., 2012. The nakhlite hydrothermal brine on Mars. Earth Planet. Sci. Lett. 359–360, 117–123.
Bridges, J.C., et al., 2001. Alteration assemblages in Martian meteorites: implications for near-surface processes. Chronol. Evol. Mars 365–392.
Bridges, J.C., Hicks, L.J., Treiman, A.H., 2019. Carbonates on mars. Chapter 5 In: Filiberto, J., Schwenzer, S.P. (Eds.), Volatiles in the Martian Crust. Elsevier, pp. 89–118.
Carr, M.H., 1996. Accretion and Evolution of Water, Water on Mars. Oxford University Press, New York, pp. 146–169.
Carr, M.H., Head, J.W., 2010. Geologic history of mars. Earth Planet. Sci. Lett. 294 (3–4), 185–203.
Carter, J., Poulet, F., 2012. Orbital identification of clays and carbonates in Gusev crater. Icarus 219 (1), 250–253.
Clark, B.C., et al., 2007. Evidence for montmorillonite or its compositional equivalent in Columbia hills, Mars. J. Geophys. Res.: Planets 112 (E6), E06S01.
Cockell, C.S., et al., 2009. Microbial Abundance in the Deep Subsurface of the Chesapeake Bay Impact Crater: Relationship to Lithology and Impact Processes.
Cockell, C.S., et al., 2016. Habitability: a review. Astrobiology 16 (1), 89–117.
Conrad, P.G., 2014. Scratching the surface of martian habitability. Science 346 (6215), 1288–1289.
Crabaugh, M., Kocurek, G., 1993. Entrada Sandstone: an example of a wet aeolian system. Geol. Soc. London Spec. Publ. 72 (1), 103–126.
DasSarma, S., 2006. Extreme halophiles are models for astrobiology. Microbe Am. Soc. Microbiol. 1 (3), 120.
Delaney, P.T., Gartner, A.E., 1997. Physical processes of shallow mafic dike emplacement near the San Rafael Swell, Utah. Geol. Soc. Am. Bull. 109 (9), 1177–1192.
Drief, A., Schiffman, P., 2004. Very low-temperature alteration of sideromelane in hyaloclastites and hyalotuffs from Kilauea and Mauna kea volcanoes: implications for the mechanism of palagonite formation. Clays Clay Miner. 52 (5), 622–634.
Ehlmann, B.L., Edwards, C.S., 2014. Mineralogy of the martian surface. Annu. Rev. Earth Planet. Sci. 42, 291–315.
Ehlmann, B.L., Mustard, J.F., 2012. An in-situ record of major environmental transitions on early Mars at Northeast Syrtis major. Geophys. Res. Lett. 39 (11), L11202.
Ehlmann, B.L., et al., 2008. Orbital identification of carbonate-bearing rocks on mars. Science 322 (5909), 1828–1832.
Filiberto, J., 2017. Geochemistry of Martian basalts with constraints on magma genesis. Chem. Geol. 466, 1–14.
Filiberto, J., Schwenzer, S.P., 2013. Alteration mineralogy of Home Plate and Columbia hills—formation conditions in context to impact, volcanism, and fluvial activity. Meteorit. Planet. Sci. 48 (10), 1937–1957.
Filiberto, J., Treiman, A.H., Giesting, P.A., Goodrich, C.A., Gross, J., 2014. High-temperature chlorine-rich fluid in the martian crust: a precursor to habitability. Earth Planet. Sci. Lett. 401 (0), 110–115.
Fiori, C., Myklebust, R., Heinrich, K., Yakowitz, H., 1976. Prediction of continuum intensity in energy-dispersive X-ray microanalysis. Anal. Chem. 48 (1), 172–176.
Goudge, T.A., Mustard, J.F., Head, J.W., Fassett, C.I., Wiseman, S.M., 2015. Assessing the mineralogy of the watershed and fan deposits of the Jezero crater paleolake system, Mars. J. Geophys. Res.: Planets 120 (4), 775–808.
Griffiths, R.W., 2000. The dynamics of lava flows. Annu. Rev. Fluid Mech. 32 (1), 477–518.
Griffith, L.L., Shock, E.L., 1995. A geochemical model for the formation of hydrothermal carbonates on Mars. Nature 377 (6548), 406–408.
Griffith, L.L., Shock, E.L., 1997. Hydrothermal hydration of Martian crust: illustration via geochemical model calulations. J. Geophys. Res. 102, 9135–9143.
Hochstein, M., Browne, P., 2000. Surface manifestations of geothermal systems with volcanic heat sources. Encyclopedia Volcanoes 835–855.
Hurowitz, J.A., et al., 2006. In situ and experimental evidence for acidic weathering of rocks and soils on Mars. J. Geophys. Res. 111, E02S19.
Jolliff, B.L., et al., 2019. mars exploration rover opportunity: water and other volatiles on ancient mars. Chapter 10 In: Filiberto, J., Schwenzer, S.P. (Eds.), Volatiles in the Martian Crust. Elsevier, pp. 285–328.
Lasue, J., Clifford, S.M., Conway, S.J., Mangold, N., Butcher, F.E.G., 2019. The hydrology of mars including a potential cryosphere. Chapter 7 In: Filiberto, J., Schwenzer, S.P. (Eds.), Volatiles in the Martian Crust. Elsevier, pp. 185–246.
Lifshin, E., Ciccarelli, M.F., Bolon, R.B., et al., 1975. X-ray spectral measurement and interpretation. In: JI, G. (Ed.), Practical Scanning Electron Microscopy. Plenum, New York, pp. 263.
Magnabosco, C., et al., 2018. The biomass and biodiversity of the continental subsurface. Nat. Geosci. 11 (10), 707–717.
Mancinelli, R.L., Fahlen, T.F., Landheim, R., Klovstad, M.R., 2004. Brines and evaporites: analogs for Martian life. Adv. Space Res. 33 (8), 1244–1246.
Marion, G.M., Catling, D.C., Crowley, J.K., Kargel, J.S., 2011. Modeling hot spring chemistries with applications to martian silica formation. Icarus 212 (2), 629–642. https://doi.org/10.1016/j.icarus.2011.01.035.
McAdam, A.C., Zolotov, M.Y., Mironenko, M.V., Sharp, T.G., 2008. Formation of silica by low-temperature acid alteration of Martian rocks: physical-chemical constraints. J. Geophys. Res. 113 (E8), E08003.
McCanta, M.C., Dyar, M.D., Treiman, A.H., 2014. Alteration of Hawaiian basalts under sulfur-rich conditions: applications to understanding surface-atmosphere interactions on Mars and Venus. Am. Mineral. 99 (2–3), 291–302.
McCubbin, F.M., et al., 2009. Hydrothermal jarosite and hematite in a pyroxene-hosted melt inclusion in martian meteorite Miller Range (MIL) 03346: implications for magmatic-hydrothermal fluids on Mars. Geochim. Cosmochim. Acta 73 (16), 4907–4917.
McLennan, S.M., 2012. Geochemistry of sedimentary processes on Mars. Mars Sedimentol., SEPM Special Publication 102, 119–138.
McSween, H.Y., 2015. Petrology on mars. Am. Mineral. 100, 2380–2395.

McSween, H.Y., Grove, T.L., Wyatt, M.B., 2003. Constraints on the composition and petrogenesis of the Martian crust. J. Geophys. Res.: Planets 108, E12.
Melwani Daswani, M., Schwenzer, S.P., Reed, M.H., Wright, I.P., Grady, M.M., 2016. Alteration minerals, fluids, and gases on early Mars: predictions from 1-D flow geochemical modeling of mineral assemblages in meteorite ALH 84001. Meteorit. Planet. Sci. 51 (11), 2154–2174.
Mittlefehldt, D.W., Gellert, R., Ming, D.W., Yen, A.S., 2019. Alteration processes in Gusev crater, mars: volatile/Mobile element contents of rocks and soils determined by the spirit rover. Chapter 11 In: Filiberto, J., Schwenzer, S.P. (Eds.), Volatiles in the Martian Crust. Elsevier, pp. 329–368.
Morris, R., et al., 2001. Phyllosilicate-poor palagonitic dust from Mauna Kea Volcano (Hawaii): a mineralogical analogue for magnetic Martian dust? J. Geophys. Res. Planets 106 (E3), 5057–5083.
Morris, R.V., et al., 2006. Mössbauer mineralogy of rock, soil, and dust at Gusev crater, Mars: spirit's journey through weakly altered olivine basalt on the plains and pervasively altered basalt in the Columbia hills. J. Geophys. Res. 111, E02S13. https://doi.org/10.1029/2005JE002584.
Morris, R.V., et al., 2008. Iron mineralogy and aqueous alteration from Husband Hill through home plate at gusev crater, Mars: results from the mössbauer instrument on the spirit mars exploration rover. J. Geophys. Res. 113. https://doi.org/10.1029/2008je003201.
Morris, R.V., et al., 2010. Identification of carbonate-rich outcrops on mars by the spirit rover. Science 329 (5990), 421–424.
Mustard, J.F., et al., 2008. Hydrated silicate minerals on Mars observed by the Mars Reconnaissance Orbiter CRISM instrument. Nature 454 (7202), 305.
Mustard, J., Bramble, M.S., Kremer, C.H., Pascuzzo, A.C., 2018. Outstanding Mars and planetary science questions from returned samples collected from NE Syrtis, midway and/or Jezero Delta. Fourth Landing Site Workshop for the Mars 2020 Rover Mission.
O'Sullivan, 1981. Western slope (Western Colorado). Epis, R.C., Callender, J.F. (Eds.), New Mexico Geological Society 32nd Annual Fall Field Conference Guidebook 89–96.
Price, A., Pearson, V.K., Schwenzer, S.P., Miot, J., Olsson-Francis, K., 2018. Nitrate-dependent Iron oxidation: a potential mars metabolism. Front. Microbiol. 9 (513).
Reed, S., Ware, N., 1972. Escape peaks and internal fluorescence in X-ray spectra recorded with lithium drifted silicon detectors. J. Phys. E 5 (6), 582–583.
Rothschild, L.J., Mancinelli, R.L., 2001. Life in extreme environments. Nature 409 (6823), 1092–1101.
Ruff, S.W., Farmer, J.D., 2016. Silica deposits on Mars with features resembling hot spring biosignatures at El Tatio in Chile. Nat. Commun. 7, 13554.
Ruff, S.W., et al., 2011. Characteristics, distribution, origin, and significance of opaline silica observed by the Spirit rover in Gusev crater. Mars. J. Geophys. Res. 116, E00F23.
Salvatore, M.R., et al., 2018. Bulk mineralogy of the NE Syrtis and Jezero crater regions of Mars derived through thermal infrared spectral analyses. Icarus 301 (Supplement C), 76–96.
Schmidt, M.E., et al., 2008. Hydrothermal origin of halogens at home plate, gusev crater. J. Geophys. Res. 113, E06S12. https://doi.org/10.1029/2007JE003027.
Schulze-Makuch, D., et al., 2007. Exploration of hydrothermal targets on Mars. Icarus 189 (2), 308–324.
Schwenzer, S.P., Kring, D.A., 2009. Impact-generated hydrothermal systems capable of forming phyllosilicates on Noachian Mars. Geology 37 (12), 1091–1094.
Schwenzer, S.P., Kring, D.A., 2013. Alteration minerals in impact-generated hydrothermal systems – exploring host rock variability. Icarus 226 (1), 487–496. https://doi.org/10.1016/j.icarus.2013.06.003.
Semprich, J., Schwenzer, S.P., Treiman, A.H., Filiberto, J., 2019. Phase equilibria modeling of low-grade metamorphic martian rocks. J. Geophys. Res. Planets 124 (3), 681–702.
Staudigel, H., Hart, S.R., 1983. Alteration of basaltic glass: mechanisms and significance for the oceanic crust-seawater budget. Geochim. Cosmochim. Acta 47 (3), 337–350.
Stroncik, N.A., Schmincke, H.-U., 2002. Palagonite – a review. Int. J. Earth Sci. 91 (4), 680–697.
Sutter, B., McAdam, A.C., Mahaffy, P.R., 2019. Volatile detections in gale crater sediment and sedimentary Rock: results from the mars science laboratory's sample analysis at mars instrument. Chapter 12 In: Filiberto, J., Schwenzer, S.P. (Eds.), Volatiles in the Martian Crust. Elsevier, pp. 369–392.
Tosca, N.J., McLennan, S.M., 2009. Experimental constraints on the evaporation of partially oxidized acid-sulfate waters at the martian surface. Geochim. Cosmochim. Acta 73 (4), 1205–1222.
Treiman, A.H., Barrett, R., Gooding, J., 1993. Preterrestrial aqueous alteration of the Lafayette(SNC) meteorite. Meteoritics 28 (1), 86–97.
Treiman, A.H., et al., 2016. Mineralogy, provenance, and diagenesis of a potassic basaltic sandstone on Mars: CheMin X-ray diffraction of the Windjana sample (Kimberley area, Gale crater). J. Geophys. Res. Planets 121 (1), 75–106.
Wang, A., et al., 2008. Light-toned salty soils and coexisting Si-rich species discovered by the Mars Exploration Rover Spirit in Columbia hills. J. Geophys. Res. 113.
Wannamaker, P.E., Hulen, J.B., Heizler, M.T., 2000. Early Miocene lamproite from the Colorado Plateau tectonic province, southeastern Utah, USA. J. Volcanol. Geotherm. Res. 96 (3), 175–190.
Westall, F., et al., 2015. Biosignatures on mars: what, where, and how? Implications for the search for martian life. Astrobiology 15 (11), 998–1029.
Williams, R.M.E., et al., 2013. Martian fluvial conglomerates at Gale crater. Science 340 (6136), 1068–1072.
Wright, J., Dickey, D., Snyder, R., Craig, L., Cadigan, R., 1979. Measured stratigraphic sections of Jurassic San Rafael Group and adjacent rocks in Emery and Sevier Counties. Utah: US Geological Survey Open-File Report. pp. 79–1317.
Yen, A.S., et al., 2008. Hydrothermal processes at gusev crater: an evaluation of paso robles class soils. J. Geophys. Res. Planets 113 (E6).
Zolotov, M.Y., Mironenko, M.V., 2007. Timing of acid weathering on Mars: a kinetic-thermodynamic assessment. J. Geophys. Res. 112 (E7), E07006. https://doi.org/10.1029/2006je002882.
Zolotov, M.Y., Mironenko, M.V., 2016. Chemical models for martian weathering profiles: insights into formation of layered phyllosilicate and sulfate deposits. Icarus 275 (Supplement C), 203–220. https://doi.org/10.1016/j.icarus.2016.04.011.